

# Synthesis and Luminescent Properties of Iridium Complexes with Reduced Concentration Quenching Effect

ZHANG Li-ying<sup>1\*</sup>, LI Bin<sup>2</sup> and WANG Jian-xing<sup>1</sup>

1. College of Science, Henan University of Technology, Zhengzhou 450001, P. R. China;

2. Key Laboratory of Excited State Processes, Changchun Institute of Optics, Fine Mechanics and Physics, Chinese Academy of Sciences, Changchun 130033, P. R. China

**Abstract** Three novel cyclometalated ligands 1-benzyl-2-phenyl-1*H*-benzoimidazole(BPBM), 1-(4-methoxy-benzyl)-2-(4-methoxy-phenyl)-1*H*-benzoimidazole(MBMPB) and 4-[2-(4-dimethylamino-phenyl)-benzoinidazol-1-ylmethyl]-phenyl-dimethyl-amine(DBPA) were designed and synthesized, and the corresponding highly efficiency green-emitting phosphorescent iridium complexes Ir(BPBM)<sub>2</sub>(acac)(**1**), Ir(MBMPB)<sub>2</sub>(acac)(**2**) and Ir(DPBA)<sub>2</sub>(acac)(**3**) with acetylacetonate(acac) as auxiliary ligand were also synthesized. The ligands are functionalized by bulky non-planarity substituents, thus the phosphorescent concentration quenching is substantially suppressed, and all the complexes exhibit bright photoluminescence(PL) in solid state. The photo-physical properties of the three iridium complexes were researched in detail. The results indicate that they have potential application in fabricating non-doped electrophosphorescence device.

**Keywords** Green-emitting; Iridium complex; Bulky non-planarity substituent

## 1 Introduction

Organic light-emitting diodes(OLEDs) that use phosphorescent complexes as emitting materials are currently being keenly pursued<sup>[1–5]</sup>. Particularly, iridium-based emitters are considered to be the seminal generation of phosphorescence emitters due to their high photoluminescence(PL) and electroluminescence(EL) efficiencies. Although OLEDs are becoming increasingly successful as a new display technology, unfortunately, phosphorescence-based emitters have some intrinsic disadvantages, such as concentration quenching and triplet-triplet(T-T) annihilation, which make them either weakly emissive or unemissive in solid state<sup>[6,7]</sup>. Consequently, the host-guest doped emitter system becomes a universal method for solving the problem of these phosphorescent materials when applied in OLEDs. Dopant molecules are dispersed and isolated in the host materials and thus concentration quenching can be avoided. However, realistically, doped OLEDs are relatively difficult to practically use because the reproducibility of the optimum doping level requires careful manufacturing control and the prolonged operation of the devices may lead to the phase separation of the guest and host materials<sup>[8]</sup>.

A solution to these drawbacks of the phosphorescence OLEDs, either in material or device, is highly needed. Recently, many researchers have turned to explore the possibility of new phosphor materials which can be vacuum-deposited into pure films(for non-doped device) with highly luminescent

efficiency<sup>[9–14]</sup>. Moreover, the performances of these recent reported non-doped phosphorescent OLEDs are comparable with, or better than, the doped OLEDs reported to date<sup>[14]</sup>. Their easy fabrication and good performance make non-doped OLEDs attractive for future mass-production processes.

In this work, we attempted to synthesize three novel cyclometalated ligands, 1-benzyl-2-phenyl-1*H*-benzoimidazole(BPBM), 1-(4-methoxy-benzyl)-2-(4-methoxy-phenyl)-1*H*-benzoimidazole(MBMPB) and 4-[2-(4-dimethylamino-phenyl)-benzoinidazol-1-ylmethyl]-phenyl-dimethyl-amine(DBPA), and the corresponding highly efficiency green-emitting phosphorescent iridium complexes Ir(BPBM)<sub>2</sub>(acac)(**1**), Ir(MBMPB)<sub>2</sub>(acac)(**2**) and Ir(DPBA)<sub>2</sub>(acac)(**3**). We designed the molecules with bulky non-planarity substituents, due to which the phosphorescent concentration quenching in solid state can be substantially suppressed. As our anticipation, all the iridium complexes exhibit highly-efficiency phosphorescent emission in solid state. We discussed their PL properties in detail, which indicates that it has potential application in non-doped OLEDs.

## 2 Experimental

### 2.1 Synthesis

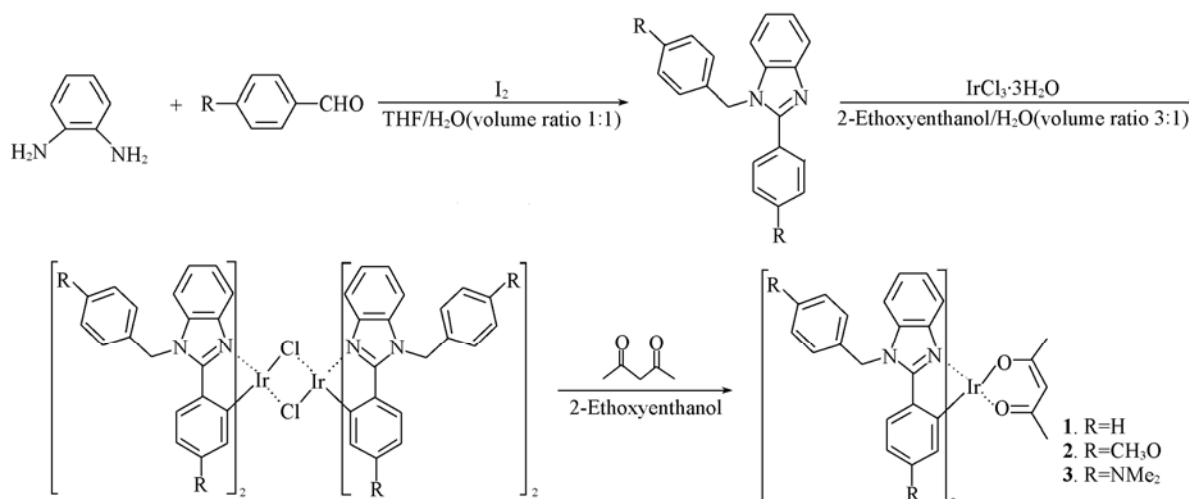
The chemical structures and synthetic routes of complexes **1–3** are depicted in Scheme 1.

\*Corresponding author. E-mail: zhangly1103@yahoo.com.cn

Received January 6, 2013; accepted March 18, 2013.

Supported by the Basic Research Foundation of Henan University of Technology, China(No.11JCYJ17) and the Science Foundation of Henan University of Technology, China(No.2009BS036).

© Jilin University, The Editorial Department of Chemical Research in Chinese Universities and Springer-Verlag GmbH



**Scheme 1** Synthetic routes of ligands and complexes 1—3

### 2.1.1 Synthesis of Ligands

The synthetic procedures of ligands are similar to the previously published ones with some minor modification<sup>[15]</sup>. For simplification, the synthesis of BPBM, as an example, is described in detail as below.

1,2-Phenylenediamine (10.0 mmol), benzaldehyde (20.0 mmol), and iodine (0.2 mmol) were dissolved in 20 mL of THF/H<sub>2</sub>O (volume ratio 1:1). The resulting mixture was stirred at 80 °C for 5 h, then extracted with CH<sub>2</sub>Cl<sub>2</sub> and purified by column chromatography on a silica gel column eluted with ethyl acetate/petroleum ether (volume ratio 1:10) to yield a white powder. Yield 2.414 g (85%). <sup>1</sup>H NMR (CDCl<sub>3</sub>, 300 MHz),  $\delta$ : 5.467 (s, 2H), 7.112 (d, 2H), 7.310 (m, 2H), 7.346 (m, 2H), 7.458 (m, 4H), 7.692 (d, 2H).

MBMPB: yield 2.752 g (80%). <sup>1</sup>H NMR (CDCl<sub>3</sub>, 300 MHz),  $\delta$ : 3.785 (s, 3H), 3.843 (s, 3H), 5.388 (s, 2H), 6.850 (d, 2H), 6.959 (d, 2H), 7.039 (d, 2H), 7.230 (m, 2H), 7.268 (d, 2H), 7.625 (d, 2H).

DPBA: yield 2.59 g (70%). <sup>1</sup>H NMR (CDCl<sub>3</sub>, 300 MHz),  $\delta$ : 2.929 (s, 6H), 3.006 (s, 6H), 5.375 (s, 2H), 6.680 (m, 2H), 6.733 (d, 2H), 7.019 (d, 2H), 7.199 (d, 2H), 7.639 (d, 2H), 7.827 (d, 2H).

### 2.1.2 Synthesis of Iridium Complexes

In a flask containing IrCl<sub>3</sub>·3H<sub>2</sub>O (243 mg, 0.68 mmol) and 1.70–2.04 mmol of each cyclometalated ligand was added a 3:1 (volume ratio) mixture of 2-ethoxyethanol and water (25 mL). In N<sub>2</sub> atmosphere, the mixture was refluxed for 48 h and then cooled to room temperature. A small quantity of water was added to precipitate an orange solid. Then the precipitate was washed with ethanol and hexane several times. The dried chloro-bridged dimer was mixed with anhydrous sodium carbonate (216 mg, 2.04 mmol) in a two-neck flask. 2-Ethoxyethanol (25 mL) and Hacac (202 mg, 2.04 mmol) were added to it and the mixture was refluxed for 16 h. The solution was cooled to room temperature to which a small quantity of water was added. The colored solid was collected by filtration. The crude product was chromatographed with an appropriate eluent to produce a pure iridium complex.

Complex **1**: yield 0.446 g (75%). <sup>1</sup>H NMR (CDCl<sub>3</sub>, 300 MHz),  $\delta$ : 2.10 (d, 6H), 3.492 (m, 1H), 5.446 (s, 4H), 6.842 (d,

4H), 6.965 (m, 4H), 7.056 (m, 2H), 7.098 (m, 8H), 7.362 (d, 4H). Elemental anal. (%) calcd. for C<sub>45</sub>H<sub>37</sub>N<sub>4</sub>O<sub>2</sub>Ir: C 62.99, H 4.34, N 6.53; found: C 63.12, H 4.62, N 6.24.

Complex **2**: yield 0.478 g (72%). <sup>1</sup>H NMR (CDCl<sub>3</sub>, 300 MHz),  $\delta$ : 2.06 (d, 6H), 3.504 (m, 1H), 3.698 (s, 6H), 3.704 (s, 6H), 5.468 (s, 4H), 6.623 (d, 4H), 6.764 (d, 4H), 6.972 (d, 2H), 7.045 (m, 4H), 7.113 (d, 4H), 7.362 (d, 4H). Elemental anal. (%) calcd. for C<sub>49</sub>H<sub>45</sub>N<sub>4</sub>O<sub>6</sub>Ir: C 60.17, H 4.64, N 5.72; found: C 59.76, H 4.92, N 6.03.

Complex **3**: yield 0.384 g (55%). <sup>1</sup>H NMR (CDCl<sub>3</sub>, 300 MHz),  $\delta$ : 2.12 (d, 6H), 3.045 (s, 12H), 3.124 (s, 12H), 3.552 (m, 1H), 5.462 (s, 4H), 6.460 (m, 4H), 6.892 (d, 4H), 6.943 (d, 2H), 7.240 (d, 4H), 7.803 (d, 4H), 7.990 (d, 4H). Elemental anal. (%) calcd. for C<sub>53</sub>H<sub>57</sub>N<sub>8</sub>O<sub>2</sub>Ir: C 61.78, H 5.58, N 10.88; found: C 62.04, H 5.92, N 10.56.

## 2.2 Apparatus

<sup>1</sup>H NMR spectra were recorded on a Bruker Avance 300 MHz spectrometer with tetramethylsilane (TMS) as the internal standard. Element analyses were performed with a Vario element analyzer. The UV-Visible absorption spectra were obtained on a Shimadzu-UV-3101 scanning spectrophotometer. Solid state PL spectra were measured with a RF-5301Pc spectrofluorophotometer. The PL decays of these complexes in the solutions excited by laser pulse at wavelength 355 nm were measured on a Quanta Ray DCR-3 pulsed Nd: YAG laser system. The voltammograms were recorded in CH<sub>3</sub>CN sample solutions of ~10<sup>-4</sup> mol/L each of complexes **1**, **2** and **3**, with 0.1 mol/L tetra-*n*-butylammonium hexafluorophosphate (TBAP) as the supporting electrolyte. Prior to each electrochemical measurement, the solution was purged with nitrogen for about 10–15 min to remove the dissolved oxygen. The highest occupied molecular orbital (HOMO) and lowest unoccupied molecular orbital (LUMO) energy levels of these complexes were calculated from the onset oxidation [ $E_{\text{onset}}(\text{Ox})$ ] and reduction [ $E_{\text{onset}}(\text{Red})$ ] potentials via the following formula  $E_{\text{HOMO}} = -4.74 - E_{\text{onset}}(\text{Ox})$  [–4.74 V for saturated calomel electrode (SCE) with respect to the zero vacuum level<sup>[16]</sup>] and  $E_{\text{LUMO}} = -4.74 - E_{\text{onset}}(\text{Red})$  respectively, as shown in Table 1.

**Table 1** Typical PL characteristics of complexes 1—3

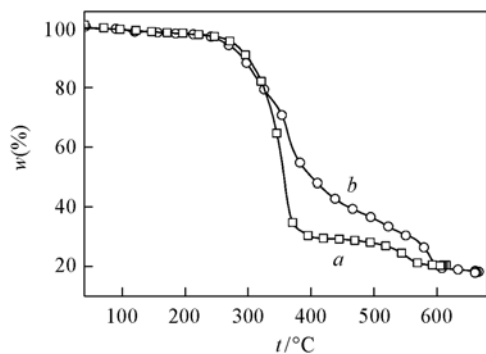
Complex	$\lambda_{\text{em}}^{\text{max } a}/\text{nm}$	$\tau^b/\text{ns}$	$\Phi^b$	$10^{-7}K_{\text{rad}}$	$10^{-6}K_{\text{nr}}$	$E_{\text{HOMO}}^c/\text{eV}$	$E_{\text{LUMO}}^d/\text{eV}$
1	517, 540	97.6	0.36	36.8	6.52	5.70	3.22
2	492, 526	84.3	0.59	70	7.86	5.74	3.12
3	510, 540	50.2	0.51	1.02	9.72	5.68	3.11

*a.* Measured in solid state; *b.* measured in dichloromethane solution,  $c=1.0 \times 10^{-5}$  mol/L; *c.* determined from the onset potential; *d.* determined from the onset reduction potential.

### 3 Results and Discussion

#### 3.1 Thermal Property

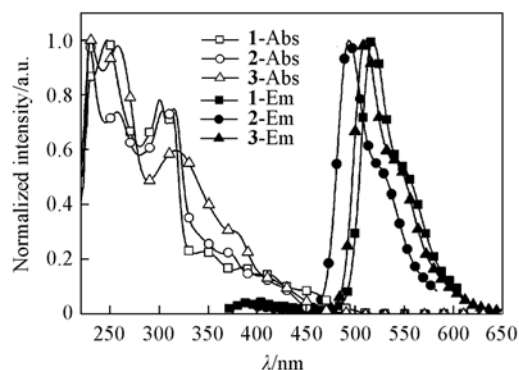
In order to examine whether these complexes are suitable for making EL devices by vacuum deposition method, the decomposition temperature were determined from the TGA curves of complexes **1** and **2** measured under nitrogen stream, as shown in Fig.1. From the thermogravimetric analysis(TGA) curves of these complexes, we can find that the temperatures of the two complexes at which the mass loss reached to 10% are 302 °C for complex **1** and 294 °C for complex **2**, respectively. The TGA curve of complex **1** shows two regions of mass loss. When temperature increases to 273 °C, complex **1** begins to dramatically disassociate, which can be assigned to the leaving of the two cyclometalated ligands BPBM(theoretical mass loss 66.04%, observed 69.46%). The second gradual mass loss with an endothermic process centered at 475 °C between 417 °C and 576 °C is due to the release of the auxiliary acac ligand. Complex **2** shows the similar thermal characteristics as complex **1**, it exhibits the first endothermic mass loss due to the release of cyclometalated ligand MBMPB at a temperature of 258 °C, and then the second endothermic mass loss due to the cleavage of the auxiliary acac ligand. The results indicate that thermostability of the two complexes is good, which makes the devices fabricated by vacuum evaporation more feasibly.

**Fig.1** TGA curves of complexes 1(a) and 2(b)

#### 3.2 Photophysical Properties

Fig.2 shows comparison of absorption spectra in dichloromethane solution and the emission spectra of complexes **1—3** in solid state. The absorption and emission spectral data of complexes **1—3** along with lifetime( $\tau$ ), emission quantum yield( $\Phi$ ), radiative transition rate( $K_{\text{rad}}$ ) and nonradiative decay rate( $K_{\text{nr}}$ ) are summarized in Table 1. All the absorption spectra of these complexes display intense multiple absorption bands which appear in ultraviolet region of the spectrum between 220 and 350 nm. The measured energies and extinction coefficients are comparable to those of the free cyclometalated ligands.

Hereby, these features are assigned to the spin-allowed  $\pi-\pi^*$  transition of the cyclometalated ligands. Both singlet metal-ligand charge-transfer( $^1\text{MLCT}$ ) and triplet MLCT( $^3\text{MLCT}$ ) bands were typically observed for these complexes. For example, complex **1** shows weak and broad absorption bands in the wavelength region of longer than 370 nm. According to the previous paper<sup>[17]</sup>, these weak bands located at long wavelengths have been assigned to the MLCT transitions of iridium complexes. Thus, the broad absorption shoulders at 414 and 456 nm observed for complex **1** are likely ascribed to the  $^1\text{MLCT}$  and  $^3\text{MLCT}$ . By analogy, complexes **2** and **3** also exhibit obviously  $^1\text{MLCT}$  and  $^3\text{MLCT}$  absorption bands, and the energies of the triplet MLCT absorption for complexes **1—3** are very similar to each other, with  $\lambda_{\text{max}}$  values ranging from 420 nm to 460 nm. The similarity of MLCT energies of these complexes is not surprising, since all the three complexes have MLCT states involving the same(pyridyl) acceptors.

**Fig.2** Comparison of absorption spectra in dichloromethane solution and emission spectra of complexes 1—3 in solid state

From the PL spectra it can be seen that complexes **1—3** all exhibit bright green emission in solid state, and show similar structural features in their emission spectra, with emission maximum at *ca.* 517, 492 and 510 nm and a shoulder at *ca.* 540, 526 and 540 nm, respectively. The emission spectral peaks of complexes **2** and **3** are slightly blue-shifted in comparison with that of complex **1**, which is the result of the introduction of  $-\text{OCH}_3$  or  $\text{NMe}_2$  substituent, an electron donating substituent, into the cyclometalated ligand that is considered to decrease HOMO level, and these could be confirmed by the data in Table 1.

The PL quantum yields of the complexes were measured in dilute solutions by comparing fluorescence intensities (integrated areas) of a standard sample(quinine sulfate) and the unknown sample according to the following equation:

$$\Phi_{\text{unk}} = \Phi_{\text{std}} \cdot (I_{\text{unk}}/A_{\text{unk}}) \cdot (A_{\text{std}}/I_{\text{std}}) \cdot (\eta_{\text{unk}}/\eta_{\text{std}})^2$$

where  $\Phi_{\text{unk}}$  is the luminescence quantum yield of the sample,  $\Phi_{\text{std}}=0.546$  is the luminescence quantum yield of quinine

sulfate<sup>[18]</sup>;  $I_{\text{unk}}$  and  $I_{\text{std}}$  are the integrated fluorescence intensities of the unknown sample and quinine sulfate, respectively;  $A_{\text{unk}}$  and  $A_{\text{std}}$  are the absorbance of the unknown sample and quinine sulfate at the wavelength of excitation;  $\eta_{\text{unk}}$  and  $\eta_{\text{std}}$  are the refractive indices of the corresponding solvents (pure solvents were assumed). All the complexes exhibit high solution phosphorescence quantum yields (0.36–0.51) at room temperature in nitrogen atmosphere. In addition, their absolute PL quantum yields in solid state were obtained *via* integrating sphere, which were determined to be 0.11, 0.17 and 0.19, indicating that the phosphorescent concentration quenching in the solid state could be substantially suppressed. As has been proven, the phosphorescence lifetime is another key factor for triplet-triplet annihilation. The longer the phosphorescence lifetime of the material, the more serious triplet-triplet annihilation of it. In this work, we measured the phosphorescence lifetime of complexes **1–3** in a  $\text{CH}_2\text{Cl}_2$  solution at a concentration of  $1.0 \times 10^{-5}$  mol/L. Fitted results are 97.6, 84.3, and 50.2 ns for complexes **1–3**, respectively, which shows that all the three complexes have shorter phosphorescence lifetime than the general phosphorescent iridium complexes.

From the quantum yield and lifetime values, an assumed unitary intersystem crossing efficiency, the radiative and overall nonradiative rate constants  $K_{\text{rad}}$  and  $K_{\text{nr}}$  were calculated for the complexes *via* the equations  $K_{\text{rad}} = \Phi/\tau$  and  $K_{\text{nr}} = (1-\Phi)/\tau$  (Table 1)<sup>[19]</sup>. As appear in Table 1,  $K_{\text{rad}}$  values are comparable for the investigated complexes. considering the experimental uncertainty in quantum yield and the fact that  $K_{\text{rad}}$  values should increase as the third power of the emission frequency, according to the Einstein law of spontaneous emission<sup>[20]</sup>, we guess that the emitting excited states involve the similar chromophore, which makes the measured  $K_{\text{rad}}$  values involve similar transition dipole moments for the emitting transition. And therefore their measured  $K_{\text{rad}}$  values are comparable. Otherwise,  $K_{\text{rad}}$  and  $K_{\text{nr}}$  values are larger than those of the reported iridium(III) complexes<sup>[21]</sup>.

## 4 Conclusions

We have systematically investigated three new iridium complexes. All the complexes are highly phosphorescent at ambient condition because of the introduction of bulky non-

planarity substituents. All these complexes exhibit short excited state lifetime and high PL yield, which should be advantageous to fabricating highly efficient non-doped EL devices.

## References

- [1] Adachi C., Baldo M. A., Forrest S. R., Thompson M. E., *Appl. Phys. Lett.*, **2000**, *77*, 904
- [2] Ma Y. G., Zhang H. Y., Shen J. C., Che C. M., *Synth. Met.*, **1998**, *94*, 245
- [3] Bian Z. Q., Gao D. Q., Sun C. Y., Wang K. Z., Jin L. P., Huang C. H., *Chem. Res. Chinese Universities*, **2002**, *18*(4), 466
- [4] Tsuboyama A., Iwawaki H., Furugori M., Mukaide T., Kamatani J., Igawa S., Moriyama T., Miura S., Takiguchi T., Okada S., Hoshino M., Ueno K., *J. Am. Chem. Soc.*, **2003**, *125*(42), 12971
- [5] Xin H., Li F. Y., Shi M., Bian Z. Q., Huang C. H., *J. Am. Chem. Soc.*, **2003**, *125*, 7166
- [6] Yang C. H., Fang K. H., Chen C. H., Sun I. W., *Chem. Commun.*, **2004**, 2232
- [7] Liu Y., Liu S. L., Wang Y. G., *Chem. Res. Chinese Universities*, **2010**, *26*(2), 249
- [8] Yang C. H., Tai C. C., Sun I. W., *J. Mater. Chem.*, **2004**, *14*(6), 947
- [9] Lupton J. M., Samuel I. D. W., Frampton M. J., Beavington R., Burn P. L., *Adv. Funct. Mater.*, **2001**, *11*, 287
- [10] Liu J., Chen H. B., Liu S. G., *Chem. Res. Chinese Universities*, **2012**, *28*(4), 572
- [11] Liu Z. W., Guan M., Bian Z. Q., Nie D. B., Gong Z. L., Li Z. B., Huang C. H., *Adv. Funct. Mater.*, **2006**, *16*, 1441
- [12] Ding J. Q., Gao J., Cheng Y. X., Xie Z. Y., Wang L. X., Ma D. G., Jing X. B., Wang F. S., *Adv. Funct. Mater.*, **2006**, *16*, 575
- [13] Markham J. P. J., Lo S. C., Magennis S. W., Burn P. L., Samuel I. D. W., *Appl. Phys. Lett.*, **2002**, *80*, 2645
- [14] Zhou G. C., Ho L., Wong W. Y., Wang Q., Ma D. G., Wang L. X., Lin Z. Y., Marder T. B., Beeby A., *Adv. Funct. Mater.*, **2008**, *18*, 499
- [15] Chou P. T., Chi Y., *Chem. Eur. J.*, **2007**, *13*, 380
- [16] Ashwini K. A., Samson A., *J. Chem. Mater.*, **1996**, *8*, 579
- [17] Kober E. M., Caspar J. V., Lumpkin R. S., Meyer T. J., *J. Phys. Chem.*, **1986**, *90*, 3722
- [18] Spellane P., Watts R. J., Vogler A., *Inorg. Chem.*, **1993**, *32*, 5633
- [19] Strickler S. J., Berg R. A. J., *J. Chem. Phys.*, **1962**, *37*, 814
- [20] Einstein A., *Phys. Z.*, **1917**, *18*, 121
- [21] Zhang J. P., Jin L., Zhang H. X., Bai F. Q., *Chem. J. Chinese Universities*, **2011**, *32*(12), 2885